Asian Journal of Chemistry; Vol. 38, No. 4 (2026), 1013-1019
ASIAN JOURNAL OF CHEMISTRY
https://doi.org/10.14233/ajchem.2026.35515

Synthesis, Characterisation, Computational Studies and Nonlinear Optical Properties of Cu(II), Ni(II) and Co(II) Complexes with 2-Hydroxynaphthaldehyde and 2,4-Dimethylaniline Derived Schiff Base Ligands

VED PRAKASH ARYA, ALOK KUMAR MAURYA and NITESH JAISWAL*,

Department of Chemistry, Prof. Rajendra Singh (Rajju Bhaiya) Institute of Physical Sciences for Study and Research, Veer Bahadur Singh Purvanchal University, Jaunpur-222003, India

*Corresponding author: E-mail: njchem1@gmail.com

Received: 26 December 2025 *Accepted*: 20 February 2026 *Published online*: 8 April 2026 AJC-22323

A series of transition metal complexes derived from 2-hydroxynaphthaldehyde based Schiff base ligand designed and synthesised. The Schiff base ligand **1** was prepared *via* condensation of 2-hydroxy-1-naphthaldehyde with 2,4-dimethylaniline. The corresponding complexes **2-4** of Cu(II), Ni(II) and Co(II) ions were synthesised using Schiff base ligand in 1:2 molar ratios. The synthesised ligand and its metal(II) complexes were characterised using elemental analysis, UV-Vis, FT-IR, ^{1}H NMR and mass spectrometry. Density functional theory (DFT) calculations at the B3LYP level with a basis set of 6-31G(d,p) were employed to optimize geometries, predict frontier molecular orbitals, compute HOMO–LUMO gaps and analyse electronic distribution. Non-liner optical properties of ligand and metal(II) complexes also computed using DFT method. The combined experimental and theoretical results suggest tetrahedral geometry in complex **2** and square-planar geometry in complexes **3** and **4**.

Keywords: Schiff base, Transition metal complex, DFT, HOMO-LUMO Gap, NLO.

INTRODUCTION

Since its discovery, Schiff bases have recognised as versatile ligands in coordination chemistry due to their synthetic flexibility, strong donor capabilities and potential biological applications [1,2]. Schiff bases are widely regarded as privileged ligands since they offer an incredible degree of the structural flexibility. The presence of the azomethine (–CH=N–) moiety enhances electron delocalisation and provides chelating sites for metal coordination. Their primary advantage lies in their structural flexibility, which allows for the precise fine-tuning of donor atoms, denticity and chelating potential to suit specific needs. The true potential of Schiff bases is realized through their ability to coordinate with the metal ions [3]. The resulting complexes often exhibit enhanced biological activities to nonlinear optical properties [4-6]. This enhancement is largely due to the unique synergistic effect between the metal centre and the organic framework, which stabilizes the structure and dictates its functional behaviour. Transition metal complexes of Schiff bases display remarkable catalytic, antibacterial and anticancer properties, making them important in modern medicinal and materials chemistry [7-10].

The hydroxynaphthaldehyde derivatives represent an advanced class of aldehydes with extended π-conjugation and intramolecular hydrogen bonding, which enhance the stability and planarity of resulting Schiff base ligands [11,12]. The substitution on the aromatic ring further tunes the electronic environment, affecting the metal–ligand interaction and physicochemical behaviour of the complexes [13,14].

The rational design of such metal complexes provides a predictive framework for correlating structure and activity. The density functional theory (DFT) allows exploration of metal–ligand bonding, electronic spectra and stability trends [15-17]. The Schiff base metal complexes can bind to biomolecular sites, often with higher affinity than the free ligand, due to additional coordination and hydrophobic interactions mediated by the metal centre [18]. Beyond medicine, these complexes are increasingly valued for their optical properties. Their extensive π-conjugated systems make them ideal candidates for nonlinear optical (NLO) applications [19-22].

This study reports the synthesis, spectral characterisation, computational analysis and non-liner optical properties of Co(II), Ni(II) and Cu(II) complexes with 2-hydroxynaphthaldehyde derived Schiff bases. The integration of theoretical and experimental data provides comprehensive insight into their structure–property activity relationship.

EXPERIMENTAL

All reagents and solvents used were of analytical reagent (AR) grade and were employed without further purification. The 2,4-dimethylaniline and 2-hydroxy-1-naphthaldehyde were purchased from SRL and Molychem, respectively. Metal salts, including cobalt(II) acetate tetrahydrate, nickel(II) acetate tetrahydrate and copper(II) acetate monohydrate, were procured from CDH and used as received.

The elemental analyses (C, H, N) were performed using a Thermo Scientific Flash 2000 CHNS–O elemental analyzer. The FT-IR spectra were recorded using KBr pellets on a Bruker Alpha-II FT-IR spectrophotometer in the range 4000-400 cm^{-1}. Electronic absorption spectra were recorded on an Agilent Cary 60 UV-Visible spectrophotometer over the range 200–800 nm. The ^{1}H NMR spectra were recorded on a JEOL AL-300 FT-NMR spectrometer operating at 500 MHz using DMSO-d_6 as solvent and TMS as an internal standard. High-resolution mass spectra (HRMS) were obtained on a SCIEX X500R QTOF-MS system.

Computational analysis: All quantum-chemical calculations were carried out with the Gaussian 09 suite program [23]. Geometry optimisations and vibrational frequency analyses were performed using density functional theory (DFT) with the B3LYP functional (Becke's three-parameter exchange with the Lee–Yang–Parr correlation functional) and the 6-31G (d,p) basis set [24-27]. Optimisations were carried out in the gas phase without symmetry constraints. Single-point electronic energies and molecular orbital analyses (HOMO/LUMO energies, frontier orbital compositions) were obtained at the same B3LYP/6-31G(d,p) level on the optimised geometries. Nonlinear optical properties of ligand and its metal(II) complexes were investigated using DFT method [28].

Synthesis of ligand: A solution of 2-hydroxy-1-naphthaldehyde (1.72 g, 10 mmol) was prepared in 25 mL of absolute ethanol and placed in a 100 mL round-bottom flask fitted with a reflux condenser [29]. To this solution, 2,4-dimethylaniline (1.21 g, 10 mmol) dissolved in 20 mL of ethanol was added dropwise with continuous stirring. The reaction mixture was refluxed for 3-4 h at 78-80 ºC (**Scheme-I**). After completion, the reaction mixture was cooled at room temperature and the resulting yellow colour precipitate was filtered, washed with cold ethanol and dried under vacuum over anhydrous $CaCl_2$.

(*E*)-1-(((2,4-Dimethylphenyl)imino)methyl)naphthalen-2-ol (1): Yield: 81%; m.f.: $C_{19}H_{17}NO$; m.w.: 275.34; Elemental analysis: calcd. (found) %: C, 82.88 (82.01); H, 6.22 (5.96); N, 5.09 (4.85); ^{1}H NMR (500 MHz, DMSO-d_6, δ_H, ppm): O-**H** 11.2, -**H**C=N 9.15, Ar-**H** 8.04-6.89, C**H**$_3$ 2.37; FT-IR (KBr, cm^{-1}): 3456ν (O-H), 2911 ν(C=C), 1625 ν(C=N), 1252 ν(C-O); UV-Vis ($CHCl_3$) (λ_{max}, nm): 280, 345, 411; TOF-MS, calcd. (found): 275.34 (275.11).

Synthesis of metal complexes: The transition metal(II) complexes of the synthesised Schiff base ligand derived from 2-hydroxy-1-naphthaldehyde and 2,4-dimethylaniline were synthesised by direct complexation under reflux in ethanol. The ligand **1** (1.10 g, 4 mmol) was dissolved in 20 mL of hot ethanol and added to ethanolic solution of copper(II) acetate monohydrate (0.39 g, 2 mmol). The reaction mixture was refluxed for 8-10 h at 80 ºC. A dark brown solid complex obtained was filtered, washed several times with ethanol. This dried under vacuum over anhydrous $CaCl_2$ (**Scheme-I**). Similar procedure was followed to synthesize nickel and cobalt complexes [30].

[CuL$_2$] (2): Yield: 69%; m.f.: $C_{38}H_{32}N_2O_2Cu$; m.w.: 612.22; Elemental analysis: calcd. (found) %: C, 74.55 (73.56); H, 5.27 (5.02); N, 4.58 (4.11); FT-IR (KBr, cm^{-1}): 2924 ν(C=C), 1604 ν(C=N), 1278 ν(C-O), 590 ν(Cu-O), 482 ν(Cu-N); UV-Vis ($CHCl_3$) (λ_{max}, nm): 291, 350, 415, 524; TOF-MS *m/z* calcd. (found) = 612.22 (611.85).

[NiL$_2$] (3): Yield: 77%; m.f.: $C_{38}H_{32}N_2O_2Ni$; m.w.: 607.37; Elemental analysis: calcd. (found) %: C, 75.15 (74.25); H, 5.31 (5.04); N, 4.61 (4.13); FT-IR (KBr, cm^{-1}): 2936 ν(C=C), 1610 ν(C=N), 1272 ν(C-O), 584 ν(Cu-O), 471 ν(Cu-N); UV-Vis ($CHCl_3$) (λ_{max}, nm): 287, 355, 419, 535; TOF-MS *m/z* calcd. (found) = 607.37 (607.02).

[CoL$_2$] (4): Yield: 72%; m.f.: $C_{38}H_{32}N_2O_2Co$; m.w.: 607.61; Elemental analysis: calcd. (found) %: C, 75.12 (74.62); H, 5.31 (5.08); N, 4.61 (4.09); FT-IR (KBr, cm^{-1}): 2941 ν(C=C), 1612 ν(C=N), 1274 ν(C-O), 579 ν(Cu-O), 460 ν(Cu-N); UV-Vis ($CHCl_3$) (λ_{max}, nm): 283, 350, 429, 542; TOF-MS *m/z* calcd. (found) = 607.61 (607.12).

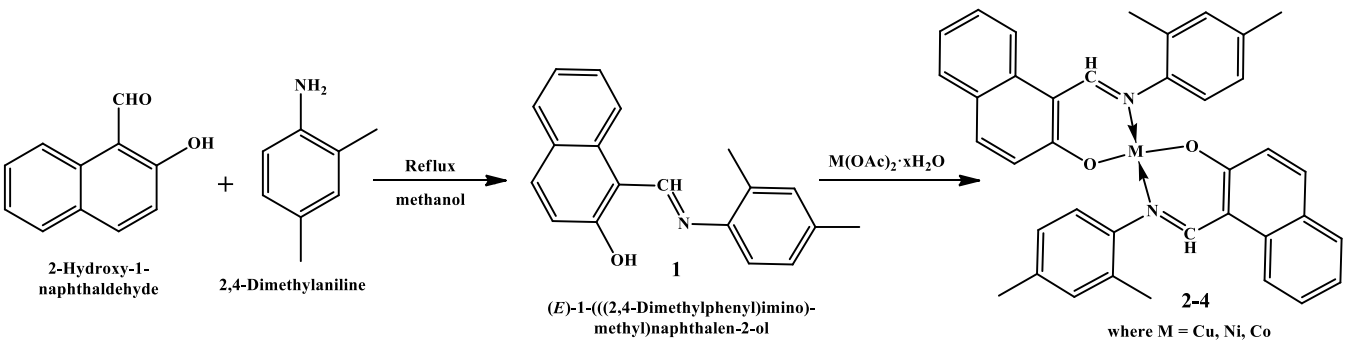

Scheme-I: Synthesis of 2-hydroxynaphthaldehyde and 2,4-dimethylaniline derived Schiff base ligands and its metal complexes

RESULTS AND DISCUSSION

UV-Vis spectral studies: The UV-Vis spectral features of the synthesised Schiff base **1** and its metal(II) complexes **2-4** provide important evidence for chromophoric changes associated with coordination. The ligand displays two major absorption bands at 280 (π→π*) and 365 nm (n→π*) regions, originating from the conjugated naphthyl ring and azo-methine group, respectively. These transitions are consistent with previously reported naphthaldehyde-derived Schiff bases [21].

Upon complexation, the n→π* transition shifts slightly toward longer wavelengths for metal complexes, indicating a decrease in imine bond order due to electron donation to the metal ion. The complexes exhibit absorptions in the 430-450 nm region assigned to ligand to metal charge transfer. The addition weak broad band in the region 524-542 nm, arising from the characteristic *d–d* transition of metal complexes [31]. A band around 524 nm in copper(II) complex can be assign to $^2T_{2g}\rightarrow{}^2E_g$ transition within tetrahedral geometry. Similarly, a weak broad band around 535 nm in nickel(II) complex and 542 nm in cobalt(II) complex suggest square planar geometry around metal ion. The shifts in the maxima wavelength and changes in absorption intensities between the ligands and their complexes confirm coordination between the ligand and metal centre through azomethine nitrogen and phenolic oxygen.

FT-IR spectral studies: The FT-IR spectra of the synthesised Schiff base **1** and its metal(II) complexes **2-4** provide clear confirmation of ligand formation and subsequent coordination. In the spectrum of Schiff base ligand **1**, a broad band around 3456 cm^{-1} is assigned to the phenolic O–H stretching mode. This band is absent in metal(II) complexes, indicating that the hydroxyl proton is lost during the metal(II) complex formation and that the phenolic oxygen participates in metal coordination [31].

The characteristic azomethine C=N stretching vibration, appearing at approximately 1625 cm^{-1} in the free ligand **1**, shifts to lower wavenumbers in the metal(II) complexes **2-4** and appear in the region 1612-1604 cm^{-1}. This downshift reflects a reduction in bond order due to electron donation from the nitrogen atom to the metal centre. Similarly, the phenolic C–O stretching band, observed near 1252 cm^{-1} in ligand, moves to higher frequency in metal complexes (1278-1272 cm^{-1}) upon chelation, supporting the involvement of oxygen in bonding [31]. The key absorptions bands of metal complexes in the region 590-579 cm^{-1} and 482-460 cm^{-1}, corresponding to M–N and M–O vibrations, respectively. These spectral observations support ligand coordination as a bidentate N, O-donor, forming stable 1:2 metal–ligand complexes [20].

NMR spectral studies: The NMR spectra of the Schiff base ligand (HL) provide clear evidence for the successful condensation between 2-hydroxynaphthaldehyde and 2,4-dimethylaniline. In the ^1H NMR spectrum**,** the phenolic –OH proton appears as a downfield singlet at δ 11.2 ppm**,** characteristic of hydrogen-bonded naphtholic groups. The azomethine –CH=N– proton resonates as a distinct singlet at δ 9.15 ppm**,** confirming the formation of imine linkage [32]. The aromatic protons of the naphthyl and substituted phenyl rings are observed in the expected region of δ 6.89-8.04 ppm, while methyl substituents on the aniline ring give singlets at δ 2.34 ppm.

Mass spectral studies: The mass spectra strongly support the proposed structures of the Schiff base ligand **1** and its metal(II) complexes **2-4**. The mass spectrum of the ligand shows a peak at *m/z* 275.11 corresponding to the molecular ion peak of ligand which matches the calculated molecular mass of 275.34 g/mol. Other fragment ions appear at lower *m/z* values, mainly arising from cleavage of the azomethine (C=N) bond and loss of one or both methyl groups from the 2,4-dimethylaniline moiety.

Copper(II) complex **2** displays a molecular ion at *m/z* 611.85 while calculated mass of for same is 612.22, whereas nickel(II) complex **3** exhibits a prominent peak at *m/z* 607.02, assignable to the molecular ion peak of complex with a calculated molecular weight of 607.37. Similarly, Co(II) complex **4** shows molecular ion peak at *m/z* 607.12 compare to calculated peak at 607.61. The mass spectral data validate the successful synthesis of the ligand and the corresponding metal(II) complexes in 1:2 molar ratios.

Computational studies: Density functional theory (DFT) calculations were carried out to understand the structural and electronic characteristics of the synthesised Schiff base ligand **1** and metal complexes **2-4**. All geometries were optimised at the B3LYP level using the 6-31G(d,p) basis set for non-metal atoms and LANL2DZ potential for the metal centers and presented in Fig. 1. The energy level diagram including HOMO-LUMO gap is depicted in Fig. 2. The calculated bond angle and bond length of ligand and metal complexes are presented in Table-1.

The calculated parameters, such as total energy, dipole moment, HOMO and LUMO energies, HOMO-LUMO gap (ΔE), chemical potential (μ), chemical hardness (η) and electrophilicity index (ω) are summarised in Table-2.

The ligand adopted a nearly planar conformation around the azomethine group, with a calculated C=N bond length of about 1.29 Å and C–O(phenolic) bond of approximately 1.43 Å. Upon coordination, Cu(II) complex **2** adopts distorted tetrahedral geometry while Ni(II) **3** and Co(II) **4** complex exhibits square planar geometry. The calculate bond lengths and bond angles are comparable with the similar type of complexes reported earlier [33]. The Cu–N and Cu–O bond length in complex **2** is approximately 1.84 Å and 1.80 Å, respectively. The calculated bond angle O17-Cu38-N58 and N20-Cu38-O39 109.0249 and 107.68, respectively. These observations support tetrahedral geometry around copper ion in complex **2**. Similarly, the characteristic bond length Ni–N, Co–N and Ni–O, Co–O found around 1.92 Å and 1.85 Å and respectively in complexes **3** and **4**. The N–Ni–O and N-Cu-O angles ranging between 88-92° and *trans* angles near 176-178°, respectively in complexes **3** and **4**. The results indicate nearly square-planar geometry around Ni and Cu ions in complexes **3** and **4**.

Frontier molecular orbital analysis revealed HOMO density distributed mainly over the phenolic oxygen, azomethine nitrogen and metal centers, while the LUMO remained largely ligand-centered, indicating intraligand π→π* transitions along with metal–ligand charge transfer. The HOMO–LUMO energy

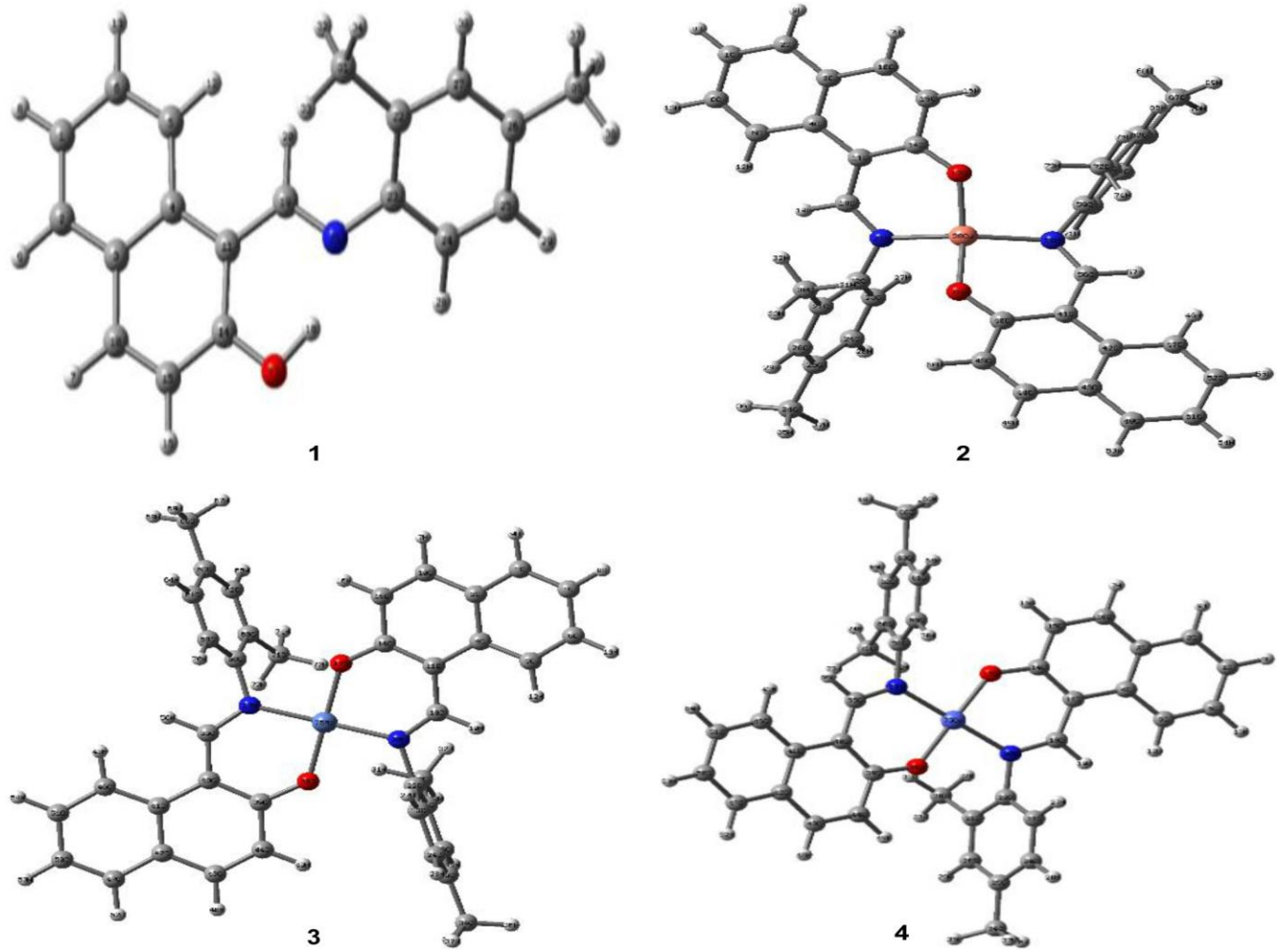

Fig. 1. Geometry optimised structures of ligand **1** and metal complexes **2-4**

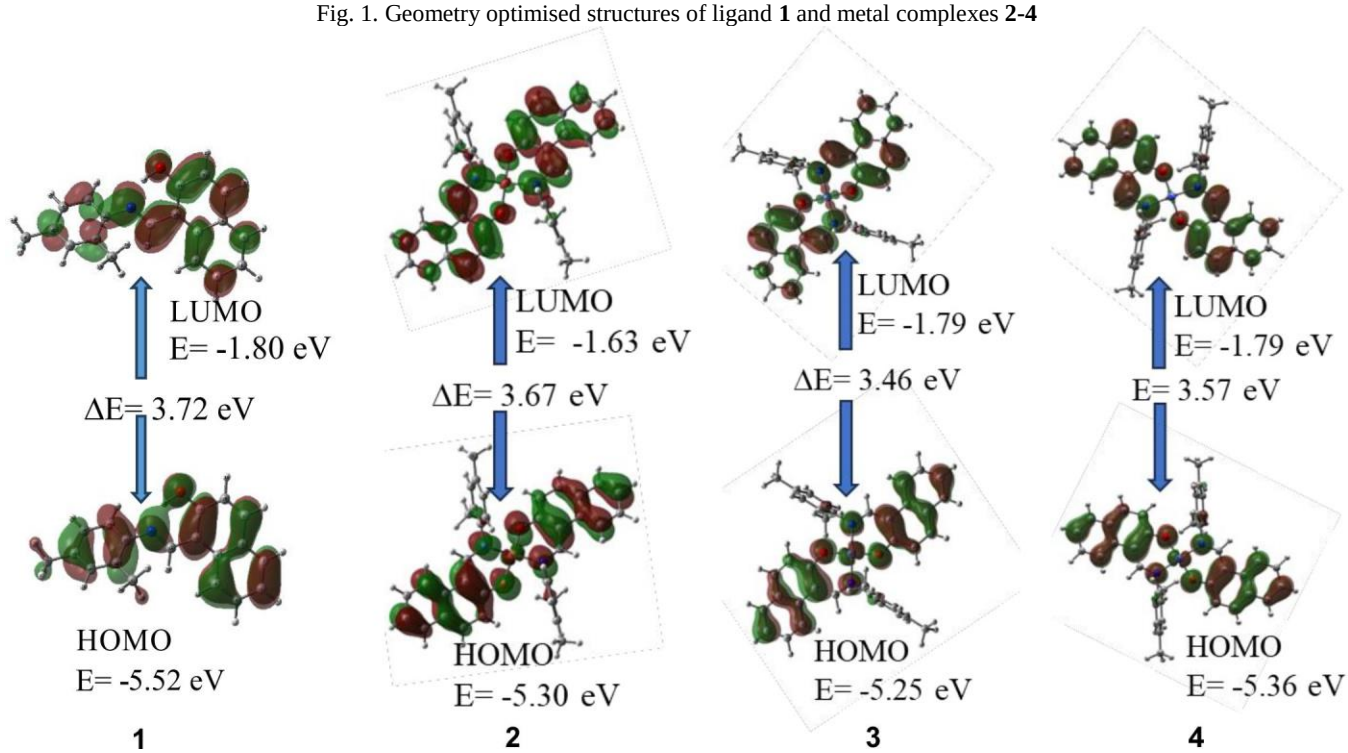

Fig. 2. Energy levels diagrams and HOMO-LUMO energy gaps of ligand **1** and its metal complexes **2-4**

TABLE-1
SOME SELECTED BOND LENGTHS (Å) AND BOND ANGLES (º) OF LIGAND **1** AND ITS METAL COMPLEXES **2-4**

Bond length (Å)							
1		**2**		**3**		**4**	
C1-C2	1.24	O17-Cu38	1.8171	O17-Ni75	1.8509	O17-Co75	1.8509
N21-C23	1.47	N20-Cu38	1.8509	N20-Ni75	1.9223	N20-Co75	1.9223
C14-O17	1.43	Cu38-O39	1.8052	O38-Ni75	1.8545	O38-Co75	1.8545
C19=N21	1.29	Cu38-N58	1.8465	N57-Ni75	1.9316	N57-Co75	1.9316
O17-H18	0.96	C56=N58	1.2868	C55=N57	1.3277	C55=N57	1.3277
Bond angle (º)							
1		**2**		**3**		**4**	
C19=N21-C23	120.00	O17-Cu38-N58	109.0249	O17-Ni75-N57	88.9725	O17-Co75-N57	88.9725
C11-C19=N21	120.00	N20-Cu38-O39	107.6845	O20-Ni75-O38	88.4111	N20-Co75-O38	88.4111
C14-O17-H18	109.47	O17-Cu38-N20	107.2215	O38-Ni75-N57	91.0527	O38-Co75-N57	91.0527
C15-C14-O17	120.00	O39-Cu38-N58	104.9461	O17-Ni75-N20	91.5663	O17-Co75-N20	91.5663
C22-C31-H34	109.47	O17-Cu38-O39	114.6445	O38-Ni75-O17	176.7615	O17-Co75-O38	178.072
–	–	N20-Cu38-N58	113.4824	N20-Ni75-O17	178.3431	N20-Co75-N57	179.250

TABLE-2
CALCULATED HOMO AND LUMO, ENERGY GAP (ΔE), CHEMICAL HARDNESS (η), ELECTRONIC CHEMICAL POTENTIAL (μ) AND ELECTROPHILICITY (ω) OF THE LIGAND **1** AND ITS METAL COMPLEXES **2-4**

Compound	Total energy	Dipole moment	HOMO	LUMO	ΔE	η	μ	ω
1	-864.04	2.8100	-5.52	-1.80	3.72	1.86	-3.66	3.60
2	-1923.28	0.8036	-5.30	-1.63	3.67	1.83	-3.46	3.27
3	-1896.46	0.4262	-5.25	-1.79	3.46	1.73	-3.52	3.58
4	-1872.24	0.5291	-5.36	-1.79	3.57	1.78	-3.57	3.57

gap decreased from ~3.72 eV in the ligand to 3.67 eV in the complex **2**, 3.46 eV in the complex **3** and 3.57 eV in complex **4** reflecting enhanced charge-transfer capability and greater reactivity upon metal coordination. Global reactivity descriptors further supported this trend, with the complex **3** showing the lowest hardness and highest electrophilicity, consistent with its greater electron-accepting ability and improved biological activity. The computational findings, together with the spectroscopic data, provide deeper insight into the electronic structure, reactivity, and stability of the complexes.

Molecular electrostatic potential (MEP): In this study, the MEP of the Schiff base ligand **1** and its metal(II) complexes **2-4** were mapped on to the total electron density surface, as illustrated in Fig. 3, where a colour-coded gradient represents the variation in electrostatic potential across the molecular framework. The regions shaded in red indicate negative potential (electron-rich zones) localised primarily around electronegative oxygen and nitrogen atoms, identifying them as favourable sites for electrophilic attack. The blue regions signify positive potential (electron-deficient zones) concentrated around hydrogen atoms, marking potential sites for nucleophilic attack. However, yellow regions indicate moderately electron-rich areas, while green regions correspond to zones of nearly neutral electrostatic potential, providing a comprehensive map of the molecules' chemical reactivity and intermolecular interaction sites.

Nonlinear optical (NLO) properties: The nonlinear optical (NLO) response of the synthesised Schiff base ligand and its metal(II) complexes was evaluated using DFT-derived polarizability and hyperpolarizability parameter. These parameters provide insight into their potential applications in photonic and optoelectronic materials [28]. The non-linear optical (NLO) properties of the Schiff base ligand **1** and complexes **2-4**, including the mean polarizability (<α>) and the first-order hyperpolarizability (β_{tot})**,** were calculated and presented in Table-3. The mean polarizability (<α>) of the free ligand was calculated to be -277.919 a.u., indicating a strong induced dipole response under an applied electric field. Upon complexation with metal, the polarizability value found as -238.223, -237.6741 and -237.8931 a.u. for complex **2**, **3** and **4**, respectively.

TABLE-3
THE B3LYP/6-31G(d, p) CALCULATED ELECTRIC DIPOLE MOMENT (debye), POLARIZABILITY (a.u.), β-COMPONENTS AND β_{tot} VALUE OF LIGAND **1** AND ITS METAL COMPLEXES **2-4**

Parameter	**1**	**2**	**3**	**4**
α_{xx}	-101.0486	-235.1369	-235.8378	-234.5576
α_{yy}	-121.3092	-224.0017	-221.0160	-222.1358
α_{zz}	-125.4507	-255.5330	-256.1687	-256.9859
α_{xy}	1.9337	5.9933	-4.9661	-4.4206
α_{xz}	1.3919	-0.0008	-0.0616	-0.4102
α_{yz}	-2.4021	0.0001	0.0981	-0.5256
<α>	-277.919	-238.223	-237.6741	-237.8931
β_{xxx}	-0.2685	0.0174	-0.4655	-0.8069
β_{xxy}	5.0061	-0.0036	-0.0284	-0.4747
β_{xyy}	9.9629	-0.0004	-0.5309	-0.1075
β_{yyy}	-22.6817	-0.0048	-1.1904	-0.0746
β_{xxz}	-8.5699	-6.6421	-38.9507	-28.1761
β_{xyz}	18.3538	-29.3784	-16.5572	-12.7323
β_{yyz}	-5.9617	0.0384	-3.4797	-4.6635
β_{xzz}	-18.2273	-6.6421	-38.9507	0.4689
β_{yzz}	3.4228	-0.0009	0.2158	0.3085
β_{zzz}	5.3877	7.6885	32.7185	21.6868
β_{tot}	18.9621	6.7132	41.1216	11.1642

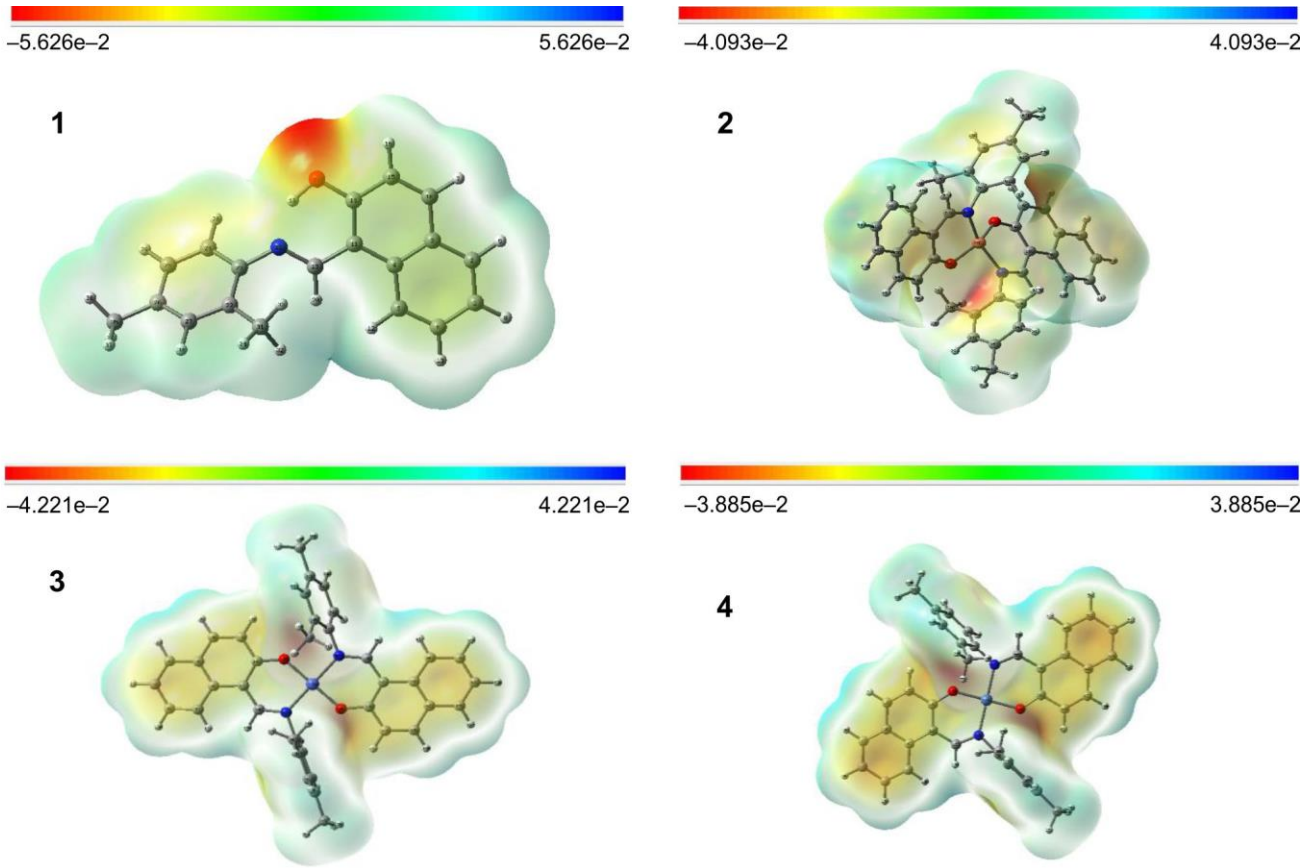

Fig. 3. MEP of ligand **1** and its metal complexes **2-4** at the B3LYP/6-31G (d,p) level of theory

The total first-order hyperpolarizability (β_{tot}), a parameter associated with second-order NLO behaviour, was found to be 18.96 a.u. for the ligand while Co(II) complex **3** shows enhanced β_{tot} value 41.12 a.u. is attributed to the presence of an extended π-conjugated system that facilitates intramolecular charge transfer (ICT). The comparison of this value with the reference compound urea (β_{tot} = 33.48 a.u.) suggests that the Ni(II) complex exhibits approximately 1.25-fold enhancement in NLO response. The enhanced β_{tot} value plays important role in tuning NLO activity of transition-metal complexes [33]. In complexes **2** and **4**, β_{tot} decreased moderately low to 6.7133 a.u. and 11.16 a.u., respectively. The calculated <α> and β_{tot} parameters demonstrated that both the ligand **1** and Co(II) complex **3** exhibit meaningful nonlinear optical responses. The Co(II) complex **3** displays a stronger NLO effect, whereas the ligand offers a slightly reduced yet still substantial response, indicating that both systems could serve as promising candidates for molecular NLO materials.

Conclusion

A Schiff base ligand (**1**) derived from 2,4-dimethylaniline and 2-hydroxynaphthaldehyde was employed for the synthesis of three transition metal(II) complexes, Cu(II), Ni(II) and Co(II) (**2-4**). The Schiff base ligand and its corresponding metal(II) complexes were characterised using elemental analysis and different spectroscopic techniques, including UV-Vis, FT-IR, NMR, mass spectrometry. The characterisation results confirm 1:2 molar ratio of metal and ligand in the complexes. The ligand acts as a monofunctional bidentate and coordinated with metal through azomethine nitrogen and phenolic oxygen. The structural analysis and DFT optimisation suggest tetrahedral geometry for Cu(II) complex **2**, while square planar geometry for Ni(II) and Co(II) complexes **3** and **4**. The Ni(II) complex displays superior NLO behaviour relative to the ligand and other metal(II) complexes.

ACKNOWLEDGEMENTS

One of the authors, (Nitesh Jaiswal), is grateful to the University Grants Commission (UGC), New Delhi, for the financial assistance through the BSR Start-up Research Grant (No. F.30-573/2021/BSR). The authors also acknowledge the Higher Education Department, Government of Uttar Pradesh, for financial support under the Research & Development Grant (vide 25/2025/361/Sattar-4-2025-003-4-(33)/2023). The authors also extend their thanks to the Centre for Advance Material Characterisation, Prof. Rajendra Singh (Rajju Bhaiya) Institute of Physical Sciences for Study and Research, Veer Bahadur Singh Purvanchal University, Jaunpur and Department of Chemistry, Institute of Science, Banaras Hindu University (BHU), Varanasi, for providing the characterisation facilities.

CONFLICT OF INTEREST

The authors declare that there is no conflict of interests regarding the publication of this article.

DECLARATION OF AI-ASSISTED TECHNOLOGIES

During the preparation of this manuscript, the authors used an AI-assisted tool(s) to improve the language. The authors reviewed and edited the content and take full responsibility for the published work.

REFERENCES

1. J. Ceramella, D. Iacopetta, A. Catalano, F. Cirillo, R. Lappano and M.S. Sinicropi, *Antibiotics*, **11**, 191 (2022); https://doi.org/10.3390/antibiotics11020191
2. P.M. Thakor, J.D. Patel, R.J. Patel, S.H. Chaki, A.J. Khimani, Y.H. Vaidya, A.P. Chauhan, A.B. Dholakia, V.C. Patel, A.J. Patel, N.H. Bhavsar and H.V. Patel, *ACS Omega*, **9**, 35431 (2024); https://doi.org/10.1021/acsomega.4c02007
3. R. Malav and S. Ray, *RSC Adv.*, **15**, 22889 (2025); https://doi.org/10.1039/D5RA03626G
4. A. Podolski-Renić, A. Čipak Gašparović, A. Valente, Ó. López, J.H. Bormio Nunes, C.R. Kowol, P. Heffeter and N.R. Filipović, *Eur. J. Med. Chem.*, **270**, 116363 (2024); https://doi.org/10.1016/j.ejmech.2024.116363
5. P. G. Lacroix, S. Di Bella and I. Ledoux, *Chem. Mater.*, **8**, 541 (1996); https://doi.org/10.1021/cm950426q
6. R.M. Ramadan, S.M. El-Medani, A. Makhlouf, H. Moustafa, M.A. Afifi, M. Haukka and A. Abdel Aziz, *Appl. Organomet. Chem.*, **35**, 6246 (2021); https://doi.org/10.1002/aoc.6246
7. M. Kumar, A.K. Singh, A.K. Singh, R.K. Yadav, S. Singh, A.P. Singh and A. Chauhan, *Coord. Chem. Rev.*, **488**, 215176 (2023); https://doi.org/10.1016/j.ccr.2023.215176
8. S. Shi, S. Yu, L. Quan, M. Mansoor, Z. Chen, H. Hu, D. Liu, Y. Liang and F. Liang, *J. Inorg. Biochem.*, **210**, 111173 (2020); https://doi.org/10.1016/j.jinorgbio.2020.111173
9. M.A. Malik, O.A. Dar, P. Gull, M.Y. Wani and A.A. Hashmi, *MedChemComm*, **9**, 409 (2018); https://doi.org/10.1039/C7MD00526A
10. X. Liu, C. Manzur, N. Novoa, S. Celedón, D. Carrillo and J.R. Hamon, *Coord. Chem. Rev.*, **357**, 144 (2018); https://doi.org/10.1016/j.ccr.2017.11.030
11. T. Bhattacharjee, S. Adhikari, A.H. Sheikh, G. Mahmoudi, S. Mlowe, M.P. Akerman, N.A. Choudhury, S. Chakraborty, R.J. Butcher, A.R. Kennedy, B.S. Demir, A. Örs and Y. Saygideger, *J. Mol. Struct.*, **1269**, 133717 (2022); https://doi.org/10.1016/j.molstruc.2022.133717
12. A. Kumar, B. Virender, B. Mohan, A.A. Solovev, M. Saini and H.K. Sharma, *Microchem. J.*, **180**, 107561 (2022); https://doi.org/10.1016/j.microc.2022.107561
13. R. Venkatesh, T. Murugan, A. Kubaib, L. Umamaheswari, P.M. Imran, M.R. AbdelGawwad, H. Alayadi and N.M. Alfrisany, *Sci. Rep.*, **16**, 2256 (2026); https://doi.org/10.1038/s41598-025-31991-2
14. A.S. Basaleh, H.B. Howsaui, A.A. Sharfalddin and M.A. Hussien, *Results Chem.*, **4**, 100445 (2022); https://doi.org/10.1016/j.rechem.2022.100445
15. S.A. Abdel-Latif and H. Moustafa, *Appl. Organomet. Chem.*, **31**, e3876 (2017); https://doi.org/10.1002/aoc.3876
16. S. Parvarinezhad, S. Ramezanipoor, M. Kubicki and M. Salehi, *Appl. Organomet. Chem.*, **38**, e7477 (2024); https://doi.org/10.1002/aoc.7477
17. A. Abdou, *Appl. Organomet. Chem.*, **39**, 7900 (2025); https://doi.org/10.1002/aoc.7900
18. S.D. Oladipo and R.C. Luckay, *New J. Chem.*, **48**, 13276 (2024); https://doi.org/10.1039/D4NJ01621A.
19. K.R. Nath Bhowmik, *Asian J. Chem.*, **36**, 2485 (2024); https://doi.org/10.14233/ajchem.2024.32594
20. T. Ashraf, A. Maryam, R. Hussain, S. Rani, B. Ali, M. Imran, S. Ashraf, U. Rahim and S.H. Sumrra, *J. Mol. Struct.*, **1323**, 140804 (2025); https://doi.org/10.1016/j.molstruc.2024.140804
21. C.E. Satheesh, P. Raghavendra Kumar, P.A. Suchetan, H. Rajanaika and S. Foro, *Inorg. Chim. Acta*, **515**, 120017 (2021); https://doi.org/10.1016/j.ica.2020.120017
22. V.K. Modanawal, S. Paswan, A. Anjum, M. Kumar, S. Srivastava and N. Jaiswal, *J. Coord. Chem.*, **74**, 3140 (2021); https://doi.org/10.1080/00958972.2021.2022128
23. M.J. Frisch, G.W. Trucks, H.B. Schlegel, G.E. Scuseria, M.A. Robb, J.R. Cheeseman, J.A. Montgomery Jr., T. Vreven, K.N. Kudin, J.C. Burant, J.M. Millam, S.S. Iyengar, J. Tomasi, V. Barone, B. Mennucci, M. Cossi, S. Scalmani, N. Rega, G.A. Petersson, H. Nakatsuji, M. Hada, M. Ehara, K. Toyota, R. Fukuda, J. Asegawa, M. Ishida, T. Nakajima, Y. Honda, O. Kitao, H. Nakai, M. Klene, X. Knox, J.E. Li, H.P. Hratchian, J.B. Cross, C. Adamo, J. Jaramillo, R. Gomperts, R.E. Stratmann, O. Yazyev, A.J. Austin, R. Cammi, C. Pomelli, J.W. Ochterski, P.Y. Ayala, K. Morokuma, G.A. Voth, P. Salvador, J.J. Dannenberg, V.G. Zakrzewski, S. Dapprich, A.D. Daniels, M.C. Strain, O. Farkas, D.K. Malick, A.D. Rabuck, K. Raghavachari, J.B. Foresman, J.V. Ortiz, Q. Cui, A.G. Baboul, S. Clifford, J. Ioslowski, B.B. Stefanov, G. Liu, A. Liashenko, P. Piskorz, I. Komaromi, R.L. Martin, D.J. Fox, T. Keith, M.A. AlLaham, C.Y. Peng, A. Nanayakkara, M. Challacombe, P.M.W. Gill, B. Johnson, W. Chen, M.W. Wong, C. Gonzalez and J.A. Pople, Gaussian 03, Revision E.01 (2009).
24. W. Kohn and L.J. Sham, *Phys. Rev.*, **140(4A)**, 1133 (1965); https://doi.org/10.1103/PhysRev.140.A1133
25. A.D. Becke, *J. Chem. Phys.*, **98**, 5648 (1993); https://doi.org/10.1063/1.464913
26. C. Lee, W. Yang and R.G. Parr, *Phys. Rev. B Condens. Matter*, **37**, 785 (1988); https://doi.org/10.1103/PhysRevB.37.785
27. B. Miehlich, A. Savin, H. Stoll and H. Preuss, *Chem. Phys. Lett.*, **157**, 200 (1989); https://doi.org/10.1016/0009-2614(89)87234-3
28. H. Moustafa, G.G. Mohamed and S. Elramly, *J. Chin. Chem. Soc. (Taipei)*, **67**, 1783 (2020); https://doi.org/10.1002/jccs.202000024
29. S. Paswan, A. Anjum, N. Yadav, N. Jaiswal and R.K.P. Singh, *J. Coord. Chem.*, **73**, 686 (2020); https://doi.org/10.1080/00958972.2020.1741557
30. M. Kumar, A. Anjum, N. Jaiswal and R.K. Dubey, *Asian J. Chem.*, **30**, 1679 (2018); https://doi.org/10.14233/ajchem.2018.21363
31. K. Jagadesh Babu, D. Ayodhya and Shivaraj, *Results Chem.*, **6**, 101110 (2023); https://doi.org/10.1016/j.rechem.2023.101110
32. S.E.A. El-Razek, S.M. El-Gamasy, M. Hassan, M.S. Abdel-Aziz and S.M. Nasr, *J. Mol. Struct.*, **1203**, 127381 (2020); https://doi.org/10.1016/j.molstruc.2019.127381
33. R.V. Sakthivel, P. Sankudevan, P. Vennila, G. Venkatesh, S. Kaya and G. Serdaroğlu, *J. Mol. Struct.*, **1233**, 130097 (2021); https://doi.org/10.1016/j.molstruc.2021.130097